

## Accepted Manuscript

Synthesis, computational studies and enzyme inhibitory kinetics of substituted methyl[2-(4-dimethylamino-benzylidene)-hydrazono)-4-oxo-thiazolidin-5-ylidene]acetates as mushroom tyrosinase inhibitors

Pervaiz Ali Channar, Aamer Saeed, Fayaz Ali Larik, Muhammad Rafiq, Zaman Ashraf, Farukh Jabeen, Tanzeela Abdul Fattah

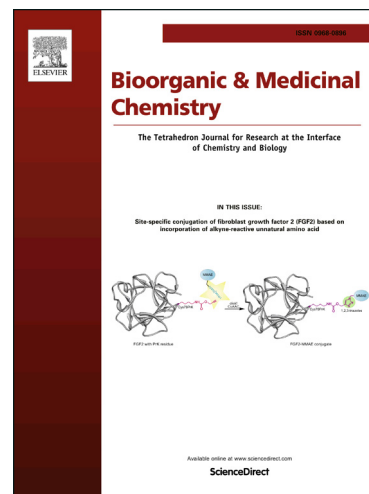
PII: S0968-0896(17)31217-8  
DOI: <http://dx.doi.org/10.1016/j.bmc.2017.09.009>  
Reference: BMC 13969

To appear in: *Bioorganic & Medicinal Chemistry*

Received Date: 9 June 2017  
Revised Date: 2 August 2017  
Accepted Date: 6 September 2017

Please cite this article as: Channar, P.A., Saeed, A., Larik, F.A., Rafiq, M., Ashraf, Z., Jabeen, F., Fattah, T.A., Synthesis, computational studies and enzyme inhibitory kinetics of substituted methyl[2-(4-dimethylamino-benzylidene)-hydrazono)-4-oxo-thiazolidin-5-ylidene]acetates as mushroom tyrosinase inhibitors, *Bioorganic & Medicinal Chemistry* (2017), doi: <http://dx.doi.org/10.1016/j.bmc.2017.09.009>

This is a PDF file of an unedited manuscript that has been accepted for publication. As a service to our customers we are providing this early version of the manuscript. The manuscript will undergo copyediting, typesetting, and review of the resulting proof before it is published in its final form. Please note that during the production process errors may be discovered which could affect the content, and all legal disclaimers that apply to the journal pertain.



**Synthesis, computational studies and enzyme inhibitory kinetics of substituted methyl[2-(4-dimethylamino-benzylidene)-hydrazono]-4-oxo-thiazolidin-5-ylidene]acetates as mushroom tyrosinase inhibitors**

Pervaiz Ali Channar<sup>a</sup>, Aamer Saeed,<sup>a,\*</sup> Fayaz Ali Larik,<sup>a</sup> Muhammad Rafiq<sup>b</sup>, Zaman Ashraf<sup>c,\*</sup>, Farukh Jabeen<sup>d,c</sup>, Tanzeela Abdul Fattah<sup>a</sup>

<sup>a</sup>Department of Chemistry Quaid-i-Azam University-45320, Islamabad, Pakistan.

<sup>b</sup>Department of Biochemistry & Biotechnology (Baghdad-ul-Jadeed Campus), The Islamia University of Bahawalpur, Bahawalpur, Pakistan,

<sup>c</sup>Department of Chemistry, Allama Iqbal Open University, Islamabad 44000, Pakistan

<sup>d</sup>Florida Center of Heterocyclic Compounds, University of Florida, Gainesville, FL, 32601, USA.

<sup>e</sup>Center for Computationally Assisted Science and Technology, North Dakota State University, Fargo, ND, 58102, USA.

**Keywords** Thiazolidinone; Synthesis; Tyrosinase Inhibitors; Kinetic Mechanism; Molecular Docking

**\* Address for Correspondence**

Aamer Saeed

Email: [asaeeed@qau.edu.pk](mailto:asaeeed@qau.edu.pk), [aamersaeed@yahoo.com](mailto:aamersaeed@yahoo.com)

Contact number: +92-51-9064-2128, Fax: +92-51-9064-2241

**\* Address for Correspondence**

Zaman Ashraf,

Email: [mzchem@yahoo.com](mailto:mzchem@yahoo.com)

Contact number: +923215194461, Fax: +92512891471

**Abstract**

The present article describes the synthesis and enzyme inhibitory kinetics of methyl[2-(arylmethylene-hydrazono)-4-oxo-thiazolidin-5-ylidene]acetates **5a–j** as mushroom tyrosinase inhibitors. The title compounds were synthesized via cyclocondensation of thiosemicarbazones **3a–j** with dimethyl but-2-ynedioate (DMAD) **4** in good yields under solvent-free conditions. The synthesized compounds were evaluated for their potential to inhibit the activity of mushroom tyrosinase. It was unveiled that compounds **5i** showed excellent enzyme inhibitory activity with  $IC_{50}$  3.17 $\mu$ M while  $IC_{50}$  of standard kojic acid is 15.91 $\mu$ M. The presence of heterocyclic pyridine ring in compound **5i** play important role in enzyme inhibitory activity as rest of the functional groups are common in all synthesized compounds. The enzyme inhibitory kinetics of the most potent derivative **5i** determined by Lineweaver-Burk plots and Dixon plots showed that it is non-competitive inhibitor with  $K_i$  value 1.5  $\mu$ M. It was further investigated that the wet lab results are in good agreement with the computational results. The molecular docking of the synthesized compounds was performed against tyrosinase protein (PDBID 2Y9X) to delineate ligand-protein interactions at molecular level. The docking results showed that the major interacting residues are His244, His85, His263, Val 283, His 296, Asn260, Val248, His260, His261 and Phe264 which are located in active binding site of the protein. The molecular modeling demonstrates that the oxygen atom of the compound **5i** coordinated with the key residues in the active site of mushroom tyrosinase contribute significantly against inhibitory ability and diminishing the human melanin synthesis. These results evident that compound **5i** is a lead structure in developing most potent mushroom tyrosinase inhibitors.

## 1. Introduction

Thiazolidin-4-ones is important scaffold in heterocyclic chemistry and the thiazolines ring is present in many pharmacological active substances. Thiazolines derivatives have a great deal of interest owing to their biological activities, such as anti-tuberculosis,<sup>1</sup> anti-convulsant,<sup>2</sup> and fungistatic<sup>3</sup> activities as well as inhibitory activity of gastrointestinal proliferation.<sup>4-5</sup> The five membered *S*- and *S,N*-heterocycles were synthesized by reacting dimethyl acetylenedicarboxylate (DMAD) with esters and amides of dithiocarboxylic acids.<sup>6-7</sup> Thioureas react with DMAD to give 1:1 adducts with loss of methanol.<sup>8</sup> A number of other more convenient methods have been reported for the preparation of thiazolidinone derivatives. For example, the reaction of thioamides or thiosemicarbazide derivatives with dialkylacetylenedicarboxylates is an effective method to prepare 2-amino-5-methoxycarbonyl-thiazolidin-4-ones.<sup>9-10</sup> Also, 2-(dimethylamino)-thiazole reacted with DMAD to produce a pyridine derivative *via* extrusion of a sulfur atom.<sup>11</sup> In recent years, the use of microwave irradiation has become popular among synthetic organic chemists, both to improve classic organic reactions (shortening reaction times and/or improving yield), and to promote new reactions.<sup>12</sup> Aly et al. demonstrated a very convenient procedure to synthesize 1,3-thiazines by the reaction of but-2-ynedioic acid, propynoic acid ethyl ester, and (*E*)-1,4-diphenyl-but-2-ene-1,4-dione with aroyl-substituted thioureas in acetic acid.<sup>13</sup> The same group changed the conditions of the reaction by mixing a solution of DEAD and aroylthioureas together with triphenyl phosphine.<sup>14</sup> The products were identified as methyl-(2*Z*)-2-[(2*Z*)-2,3-diaryl-carbonylimino-4-oxo-thiazolidin-5-ylidene]-acetates. Acylthiosemicarbazides represent versatile synthon for various syntheses of nitrogen-sulfur heterocycles. The acylthiosemicarbazide moiety provides an opportunity to perform cyclocondensations as well as addition-cyclization reactions. The products of these reactions are thiazin-2-ylidene,<sup>15</sup> thiazoline,<sup>16</sup> triazole,<sup>17</sup> and imidazolidine derivatives.<sup>18-19</sup> It has been reported that the reaction of dimethyl acetylenedicarboxylate with thiocarbamides led to 4-oxathiazolidine derivatives.<sup>20</sup>

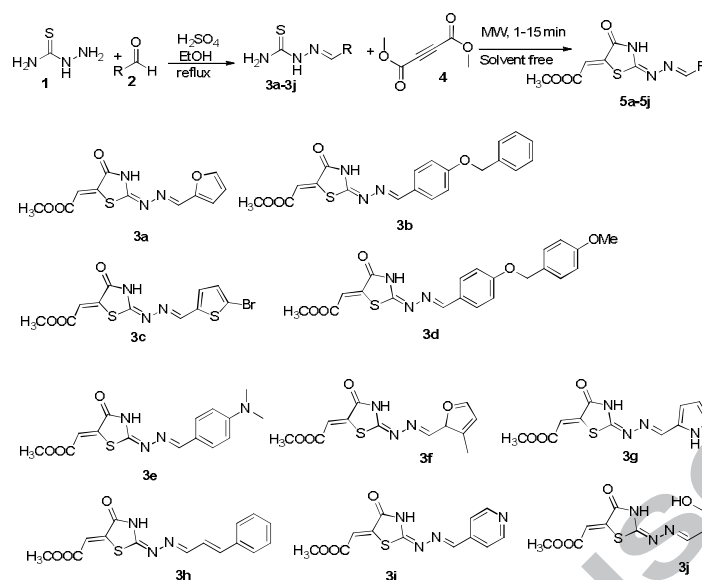
Owing to biological importance of the thiazolidinones we here describe the synthesis of title thiazolidinones **5a-j** by condensation of thiosemicarbazones with dimethyl acetylenedicarboxylate. The presence of the thiazolidinone pharmacophore as reported in previous studies, led us to investigate their mushroom tyrosinase inhibitory kinetics of the

synthesized compounds. The computational molecular docking studies has also been performed to compare the wet lab results with dry lab findings.

## 2. Results and discussion

### 2.1 Chemistry

Thiazolidinone derivatives **5a-j** were synthesized by condensation of substituted thiosemicarbazones **3a-j** with dimethyl acetylenedicarboxylate **4**. Thiosemicarbazones **3a-j** were synthesized as intermediates by acid catalyzed condensation of thiosemicarbazide with a range of substituted aromatic aldehydes (Scheme I). Thiosemicarbazones **3a-j** were then reacted with dimethyl acetylenedicarboxylate **4** in the absence of any solvent or catalyst, afforded thiazolidinones **5a-j** in good to excellent yields (Scheme I). DMAD is a highly electrophilic reagent and widely employed as a dienophile in cycloaddition reactions, such as the Diels–Alder reaction and behaving as Michael acceptor in organic transformations. The structures of **5a-j** were assigned on the basis of their FTIR,  $^1\text{H}$  and  $^{13}\text{C}$ -NMR spectral data. In the  $^1\text{H}$ -NMR spectra of **5a-j**, the down-field singlets in the region  $\delta$  13.04–8.06 ppm were assigned to NH ring proton, while the azomethine protons ( $\text{C}^2\text{thiazolH}=\text{N}$ ) appeared in the region  $\delta$  9.38–7.49 ppm. The olefinic protons ( $\text{CH}=\text{C}$ ) resonated in the region  $\delta$  6.73–6.42 ppm, while the singlets in the region  $\delta$  3.90–3.78 ppm were attributed to the protons acetoxy group. In the  $^{13}\text{C}$  NMR spectra, carbonyl carbon atoms of the thiazole ring and the acetoxy group appeared in the regions  $\delta$  174.0–170.1 ppm and  $\delta$  168.5–164.5 ppm respectively, whereas C-2 of the thiazolidinone ring resonated in the region  $\delta$  159.4–156.3 ppm. The presence of the signals in the region  $\delta$  149.6–145.2 ppm were assigned to azomethine carbon atoms attached to the aromatic rings ( $\text{ArCH}=\text{N}$ ), except those of compounds **5a** and **5i** which appeared at  $\delta$  160.3 and 158.4 ppm, respectively. Olefinic carbon atoms ( $\text{C}^5\text{thiazol}=\text{CH}$ ) were observed in the region  $\delta$  143.9–137.9 ppm, while C-5 of the thiazolidinone ring appeared in the region  $\delta$  134.6–131.1 ppm.



Scheme I. Synthesis of 1-(Substituted benzylidene thiosemicarbazides **3a-j**

## 2.2 Tyrosinase inhibitory activity

The synthesized thiazolidinones **5a-j** have been screened for their inhibitory effects on mushroom tyrosinase activity. The compound **5i** showed excellent tyrosinase inhibitory activity with  $\text{IC}_{50}$  value  $3.17\mu\text{M}$  while  $\text{IC}_{50}$  value of standard kojic acid is  $15.91\mu\text{M}$ . The presence of heterocyclic pyridine ring in compound **5i** play important role in enzyme inhibitory activity as rest of the functional groups are common in all synthesized compounds Table 1.

**Table 1** The inhibitory effects of compounds **5a-j** on mushroom tyrosinase activity.

Compounds	Tyrosinase Activity ( $\text{IC}_{50} \pm \text{SEM } \mu\text{M}$ )
<b>5a</b>	$75.26 \pm 8.2$
<b>5b</b>	$141.77 \pm 21.0$
<b>5c</b>	$348.93 \pm 33.4$
<b>5d</b>	$297.60 \pm 18.5$
<b>5e</b>	$100.45 \pm 12.6$
<b>5f</b>	$49.82 \pm 11.9$
<b>5g</b>	$50.12 \pm 9.8$

<b>5h</b>	208.25 ± 20.2
<b>5i</b>	3.17 ± 0.37
<b>5j</b>	ND
<b>Kojic acid</b>	15.91 ± 2.5

ND is not determined

### 2.3 Enzyme inhibitory Kinetics

Since **5i** was the most potent inhibitor in hand, we therefore further study mechanism underlying their inhibitory effect. The Lineweaver-Burk plot of  $1/V$  versus  $(1/[S])$  in the presence of different concentrations of **5i** gave a series of straight lines, all of which intersected at the same point on the x-axis Figure.1 (a). The analysis showed that  $1/V_{max}$  increased to a new value while that of  $K_m$  remain same in the presence of increasing concentrations of **5i**. This behavior indicated that **5i** inhibit tyrosinase non-competitively to form enzyme inhibitor (EI) Complex<sup>21</sup>. To gain insightful the pathway in which **5i** preferentially proceeded, binding affinities of EI were determined.  $K_i$  value (the constant of dissociation of the enzyme-inhibitor complex into free enzyme and inhibitor) was determined by the secondary re-plot of slope against concentration of **5i** Figure. 1(b) and by the interpretation of Dixon plot by using initial velocities at 475nm Figure 2. Kinetic constants and inhibition constants are summarized in Table 2. It was observed that compound **5i** produced same enzyme inhibition at a lower dose than the reference kojic acid which indicates its higher potency than kojic acid Figure 3.

**Table 2** Kinetic constants and inhibition constants of compound **5i** on mushroom tyrosinase

Dose	$V_{max}$ ( $\Delta A_{475nm}/Sec$ )	$K_m$ (mM)	Inhibition Type	$K_i$ ( $\mu M$ )	$IC_{50}$ ( $\mu M+SEM$ )
No inhibitor	0.01	1			
1.06 $\mu M$	$5.55 \times 10^{-4}$	1	Non-competitive	1.5	$3.17 \pm 0.37$
8.50 $\mu M$	$1.00 \times 10^{-3}$	1			
17.0 $\mu M$	$3.33 \times 10^{-3}$	1			

$V_{max}$  is the velocity of reaction.

$K_m$  is the Michaelis-Menten constant.

$K_i$  is the inhibition constant.

$IC_{50}$  is the concentration at which 50% of the enzyme activity is inhibited.

SEM is standard error of the mean.

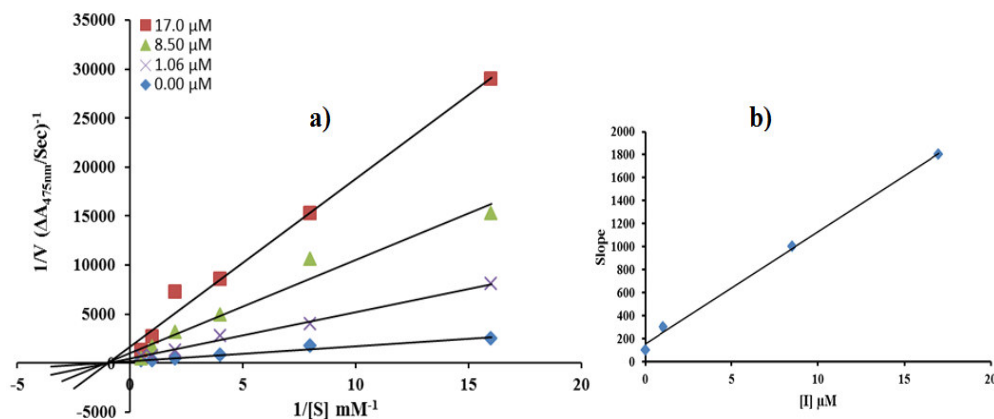


**Figure 1.** a) Lineweaver-burk plots for the inhibition of compound **5i** on mushroom tyrosinase for catalysis of L-DOPA. Inhibitor concentrations were 0.00, 1.06, 8.50 and 17.00  $\mu M$ , L-DOPA concentrations were 0.062, 0.125, 0.25, 0.5, 1 and 2 mM, respectively. b) Represents the secondary replot of slope versus concentration of compound **5i** to determine the inhibition constant ( $K_i$ ).

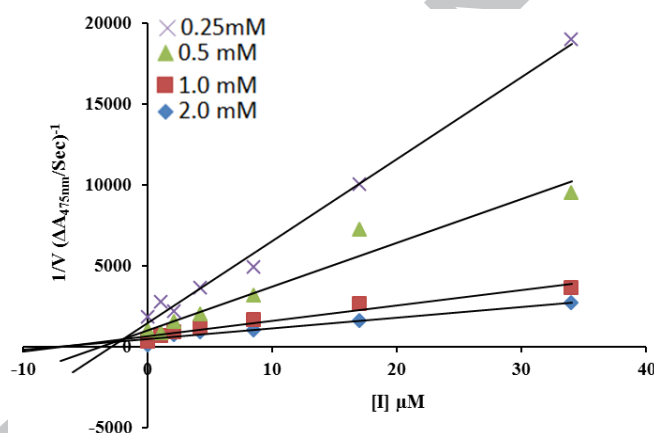


**Figure 2.** Dixon plots for the inhibition of the diphenolase activity of mushroom tyrosinase by various concentrations, 0.0, 1.06, 2.12, 4.25, 8.5, 17 and 34  $\mu M$  of compound **5i** in the presence of different concentrations of L-DOPA (0.25, 0.5, 1 and 2 mM), respectively.

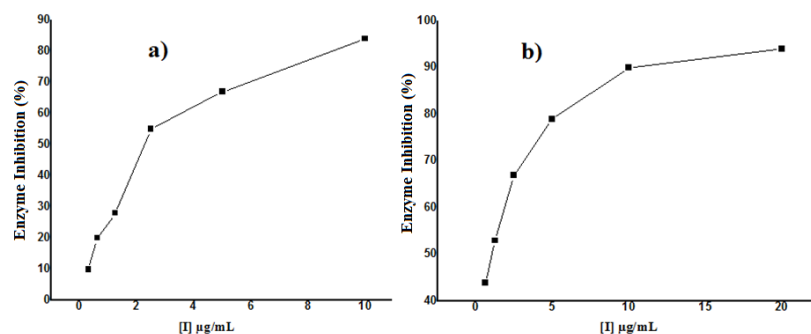


**Figure 3.** a) Effect of kojic acid and b) compound **5i** on the diphenolase activity against mushroom tyrosinase for the catalysis of L-DOPA at 25°C.

## 2.4 Docking Studies

The pharmacophore modeling and molecular docking studies has been introduced as a prevailing way complementing traditional high through put screenings. Molecular docking is an optimization problem that would define the ‘best-fit’ positioning of a compound that binds to a specific protein of interest. The molecular docking studies thus play an important role in preliminary drug research. In order to give an explanation and understanding of potent inhibitory activity observed, molecular docking was performed against mushroom tyrosinase (PDBID 2Y9X). All the docked conformations for each compounds were analyzed and it has been found that the most favorable docking poses out of 30 docked conformations for each compound, were retained to investigate the interactions of the docked conformations within the active site. All the top ranked docking conformations of synthesized compounds were stacked well inside the active site cavity. It has been reported that His 244, His 85, His263, Val 283, His 296, Asn260, Val248, His260, His261 and Phe264 are found to be key residues which are also reported in literature.<sup>22-24</sup> the active site was architecture with both the hydrophobic and hydrophilic amino acids along with the two copper ions. The hydrophobic part was constructed by, Val 283, Met280, Ala246, Phe90, Ala286, Val 248, Phe246 and His256 while hydrophilic portion contained amino acids such as His244, His279, Gly86, His61, Ser282, His 85, His 263, Gly281, Glu256, Asn260, His256, Glu322, Gly96, Ser282. Active site is a deep cavity with the wide opening and narrow end. All the preferred docked poses stacked beautifully inside the cavity. The superimposition of the best possible docked poses are shown in **Figure 4**.

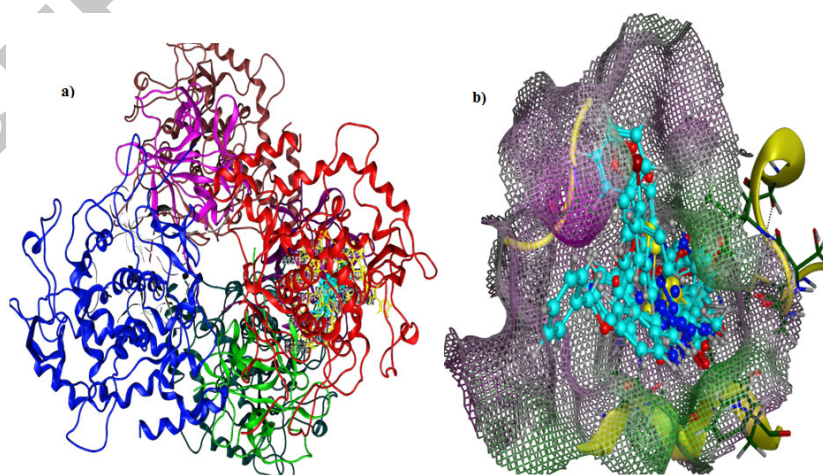


**Figure 4.** a) Overlaying of all the minimum energy docked poses inside the pocket b) Close view, (surfaces, line mode, are drawn around pocket to map the pocket). Ligands are shown in yellow color in stick mode while key residues are shown in green color in stick mode.

An insight in to the binding mode analysis of the best possible binding mode of the most preferred docked conformations revealed that ligands hydrogen bonding, hydrophobic, polar pi-pi, pi-H and cationic interaction with Copper ion at different potential. Almost all the ligands showed similar pattern of binding inside the active site. **Figure S1** showed 2-D interactions of all the ligands. The aromatic rings made similar stack of interactions with His 263, and Val283 in some ligands. Experimental results and docking results complemented each other in terms of interactions with key residues and inhibitory activity, the compounds which were found to be active in experimental studies showed multiple binding interactions while the one which showed fewer interactions showed decreased inhibitory potential. The docking model showed that **5i** applied distinct orientation to interact with the active site residues of mushroom tyrosinase. The oxygen atom of carbonyl group in compound **5i** made the close contacts with key amino acids such as His 85 and His296. **Figure 5** depicted the 3-D interaction of this ligand engaged the active-site residues, using typical hydrogen bonds to anchor tightly within the backbone of the enzyme. In addition, two hydrogen bonds were observed between the hydroxyl groups of **5i** and His85 and His296, respectively.

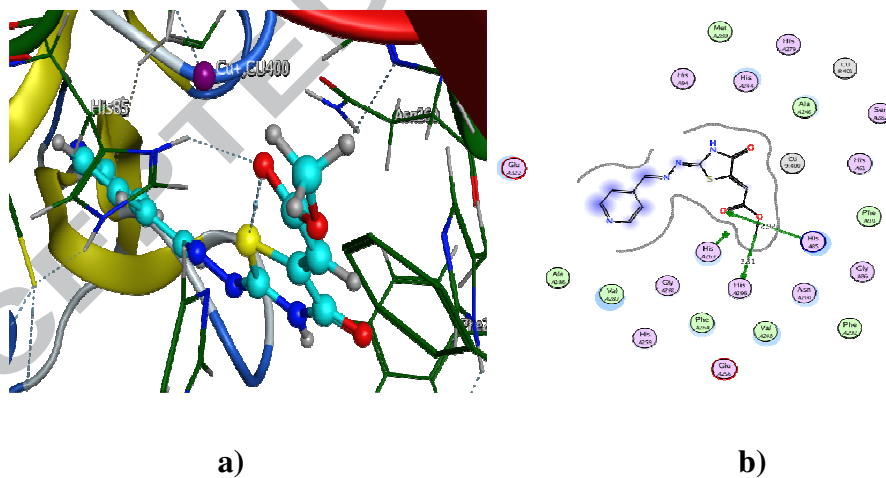


**Figure 5.** Molecular docking analyses of **5i** toward mushroom tyrosinase. (a) The docking model of molecule inside active site in 3D Interaction of ligand **5i** with active site residues. (b) 2D schematic representation of the interactions between **5i** and active site residues of mushroom tyrosinase. (The green dash lines in a and b panels donate the interactions, and the purple spheres represent two copper ions).

This indicated that the both the oxygen atom of acyl substitution of **5i** is of great potential in interacting with amino acids which are mandatory for the catalytic activities of the enzyme and significantly contributed in mushroom tyrosinase inhibition. It has also been supported by the investigation of the compounds **5g**, **5h**, **5i** and **5j** which are anchored through hydrogen bonding in active site making this an evidence that the ester substitution at the this position is imperative for inhibitory activities. The compounds **5g**, **5h**, **5i** and **5j** with ester substitution showed similar orientation pattern and established significant hydrogen bonding with the catalytic residues His 85, His296 and Asn85. Compound **5g**, **5h** and **5i** exhibited better activities ( $IC_{50}$ , 49.82, 50.12 and 3.17  $\mu\text{mol}$  respectively) as compared to the all other especially compound **5i** much better than the Kojic acid. ( $IC_{50}$  15.91  $\mu\text{mol}$ ). Compound **5j** showed almost similar binding pattern to that of compound **5i** however experimental  $IC_{50}$  is not available but predicted  $IC_{50}$  proclaimed this compound to be a potential surrogate for the tyrosinase inhibition.

Taking into account the peculiarities of the active-site residues in the tyrosinase catalysis, it can be inferred that most of the synthesized compounds made contacts with the side chains of mushroom tyrosinase His244, His 85, His263, Val 283, His 296, Asn260, Val248, His260, His261 and Phe264 residues, which was reflected in their enhanced affinity to the residues Table S1. Besides being directly involved in the architecture of the active site, the residue has a vital role in positioning other key residues in the active site appropriately for the catalysis.

### 2.5 QSAR modeling

The best multi-linear regression (BMLR)-1 was utilized which is a stepwise search for the best n-parameter regression equations (where n stands for the number of descriptors used), based on the highest  $R^2$  (squared correlation coefficient),  $R^2_{cvOO}$  (squared cross-validation “leave one-out, LOO” coefficient),  $R^2_{cvMO}$  (squared cross-validation “leave many-out, LMO” coefficient), F (Fisher statistical significance criteria) values, and  $s^2$  (standard deviation). The QSAR models up to 2 descriptor model describing the urease inhibitors against tyrosinase were generated (obeying the rule of 5:1, which is the ratio between the data points and the number of QSAR descriptor or model). The observed and predicted values of the training set compounds **5a-j** according to the multi-linear QSAR models are presented in Table 1. The established QSAR model is statistically significant. The descriptors are sorted in the descending order of the respective values of the Student's-t-criterion, which is a widely accepted measure of statistical significance of individual parameters in multiple linear regressions. **Figure 6** shows the QSAR

multi-linear model plot of correlations representing the observed vs. predicted  $IC_{50}$  values for the synthesized compounds. The scattered plots are uniformly distributed, covering ranges of  $IC_{50}$ , observed 3.17-348 and predicted 15.54-288.

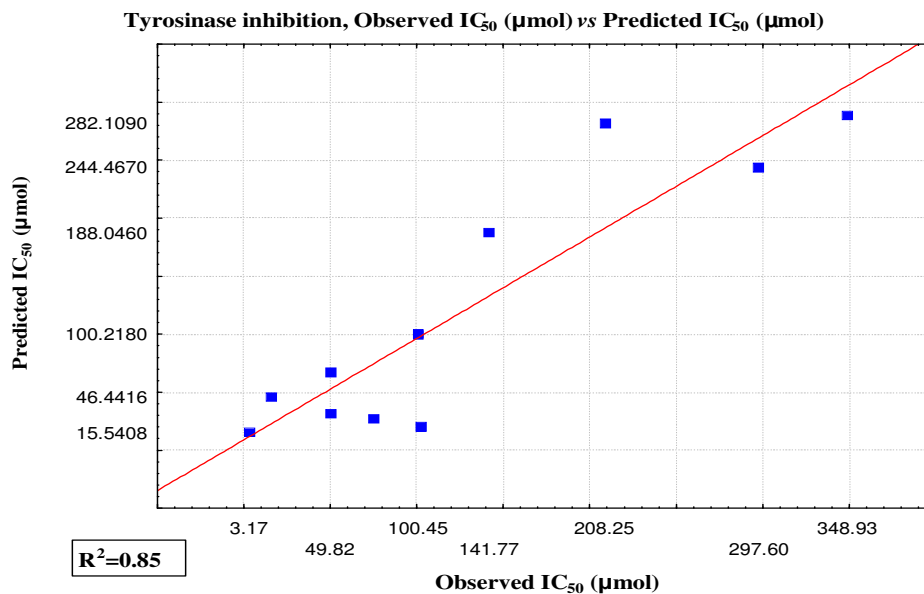


**Figure 6.** Co-relation plot of observed  $IC_{50}$  vs experimental  $IC_{50}$  (QSAR) of compounds **5a-j**.

### 2.6 Validation of 2D-QSAR model

The reliability and statistical relevance of the QSAR model is examined an internal validation procedure. The dataset contains relatively few experimental data points but is homogeneous in synthesized compounds. Therefore, application of the internal validation methodology is an appropriate technique. Internal validation is applied by the CODESSA-Pro technique employing both leave one out (LOO), which involves developing a number of models with one example omitted at a time, and leave many out (LMO), which involves developing a number of models with many data points omitted at a time (up to 20% of the total data points). The observed correlations by the internal validation technique are  $R^2_{cvLOO} = 0.72$ ,  $R^2_{cvMO} = 0.811$ , respectively which are significantly correlated with the squared correlation coefficient of the attained 2D-QSAR model ( $R^2 = 0.867$ ). Standard deviation of the regression ( $s^2 = 2354.08$ ) is also a measurable value for the attained model together with the Fisher test value ( $F = 26.709$ ) that reflects the ratio of the variance explained by the model and the variance due to their errors. A high value of the F-test relative to the  $s^2$  value is also validation of the model. The predicted/estimated tyrosinase inhibitory activity due to the attained BMLR-QSAR model of most of the synthesized compounds are compatible with their experimentally observed values

preserving their relative potencies (Table 3). The estimated/predicted  $IC_{50}$  value of compound **5e** correlated well with its observed bio-activity ( $IC_{50} = 100.45, 100.21$ ) for observed and estimated bio-properties, respectively, error = 0.23). All of above cross validation results are good indications of the predictive power of the attained 2D-QSAR model not only for validating the observed bio-data but also for optimizing high potent hits having methyl [2-(4-Dimethylamino-benzylidene)-hydrazono)-4-oxo-thiazolidin-5-ylidene]acetates scaffold.

**Table 3** Observed and predicted  $IC_{50}$  values of synthesized compounds **5a-j** against tyrosinase.

Entry	$IC_{50}$ (obs.)	$IC_{50}$ (pred.)	(error)
<b>5a</b>	75.2± 8.2	27.3281	47.9319
<b>5b</b>	141.7±21.0	188.046	-46.276
<b>5c</b>	348.3±33.4	288.612	60.3185
<b>5d</b>	297.6±18.5	244.467	53.133
<b>5e</b>	100.5±12.6	100.218	0.231663
<b>5f</b>	49.2± 11.9	67.2464	-17.4264
<b>5g</b>	50.1 ± 9.8	31.2712	18.8488
<b>5h</b>	208.2±20.2	282.109	-73.8592
<b>5i</b>	3.17± 0.37	15.5408	-12.3708
<b>5j</b>	N/A	20.9611	N/A
<b>Kojic acid</b>	15.91	46.4416	-30.5316

$IC_{50}$  is the concentration of an inhibitor required to reduce the rate of an enzymatic reaction by 50%

### 3. Conclusion

We have described the synthesis of methyl[2-(arylmethylene-hydrazono)-4-oxo-thiazolidin-5-ylidene]acetates **5a-j** via cyclocondensation of thiosemicarbazones with dimethyl but-2-ynedioate (DMAD) in good yields under solvent-free conditions. The title compounds were screened for their mushroom tyrosinase inhibitory activity, compound **5i** showed excellent activity with  $IC_{50}$  value 3.17 $\mu$ M while  $IC_{50}$  value of standard kojic acid is 15.91 $\mu$ M. The enzyme inhibitory kinetics of compound **5i** determined by Lineweaver-Burk plots and Dixon plots showed that it is non-competitive inhibitor with  $K_i$  value 1.5  $\mu$ M. The computational molecular docking performed against tyrosinase protein (PDBID 2Y9X) showed that the major interacting residues are His244, His85, His263, Val 283, His 296, Asn260, Val248, His260, His261 and Phe264 which are located in active binding site of the protein. The molecular modeling demonstrates that the oxygen atom of the compound **5i** coordinated with the key residues in the active site of mushroom tyrosinase contribute significantly against inhibitory ability and

diminishing the human melanin synthesis. These results evident that compound **5i** is a lead structure in developing most potent mushroom tyrosinase inhibitors.

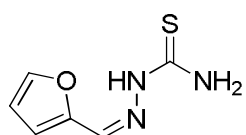
#### 4. Experimental

Melting points were recorded using a digital Gallenkamp (SANYO) model MPD.BM 3.5 apparatus and are uncorrected.  $^1\text{H-NMR}$  spectra were determined as  $\text{CDCl}_3$  solutions at 300 MHz using a Bruker AM-300 spectrophotometer using TMS as an internal reference and  $^{13}\text{C}$  NMR spectra were determined at 75 MHz using a Bruker 75 MHz NMR spectrometer in  $\text{CDCl}_3$  solution. FTIR spectra were recorded on an FTS 3000 MX spectrophotometer. Mass Spectra (EI, 70 eV) on a MAT 312 instrument, and elemental analyses were conducted using a LECO-183 CHNS analyzer.

#### General procedure for synthesis of 2-(hetero (aryl) methylene) hydrazine-1carbothioamides (Schiff bases) (3a-3j)

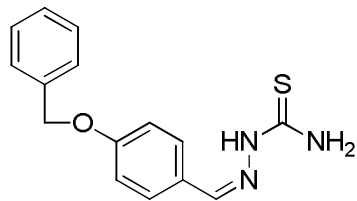
To a stirred solution of **1** (0.138 g, 1.0 mM) in 25 mL absolute ethanol, suitably substituted aldehydes or ketones (1.0 mM) along with 1–2 drops of conc. sulfuric acid were added, the mixture was refluxed for 12 h, then cooled to room temperature, and the solids obtained were filtered and recrystallized from ethanol to give compounds<sup>25,26</sup>.

#### (3a) (Z)-2-(furan-2-ylmethylene)hydrazinecarbothioamide



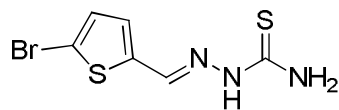
(80%): m.p 210°C  $R_f$ : 0.39; Petroleum ether : ethyl acetate (6:4) IR; (KBr,  $\text{cm}^{-1}$ ): 3374 ( $\text{NH}_2$ ), 3240 (N-H), 3125 ( $\text{sp}^2\text{CH}$ ), 1603 (C=N), 1587 (Ar-C=C), 1090 (C=S), 1053 (C-O)  $^1\text{HNMR}$ ; (300MHz, DMSO):  $\delta$  11.42 (s, 1H, NH), 8.20 (s, 1H, CH=N), 7.96 (s, 1H), 7.80 (dd,  $J = 7.6$  Hz, 1.6 Hz, 1H), 7.61 (t,  $J = 7.4$  Hz, H). 7.96 (s, 2H  $\text{NH}_2$ ),  $^{13}\text{CNMR}$  (75 MHz):  $\delta$  181.11, 148.31, 144.95, 141.59 120.79, 112.85.

#### (3b) (Z)-2-(4-(benzyloxy)benzylidene)hydrazinecarbothioamide



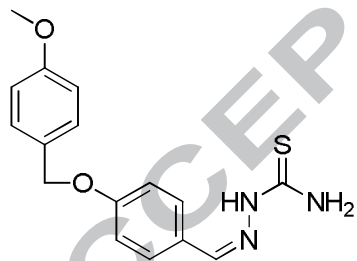
(95%), m.p 171<sup>o</sup>C; Rf: 0.53; **IR**; (KBr, cm<sup>-1</sup>): 3438 (NH<sub>2</sub>), 3305 (N-H), 1615 (CN), 1592(Ar-C=C), 1115 (C=S), cm<sup>-1</sup>; <sup>1</sup>H NMR (Acetone-d<sub>6</sub>,300 MHz) δ: 10.8 (s, 1H, NH), 8.21 (s, 1H, CH=N), 7.60-6.82 (m, 4H, ArH), 7.23 (s, 5 H, ArH), 7.1 (s, 2H, -NH<sub>2</sub>), 5.70 (s, 1H, -OCH<sub>2</sub>); <sup>13</sup>C NMR (75 MHz) δ: 179.0 (C=S), 146(C=N), 119 (Ar 2C), 122 (Ar 2C), 128 (Ar), 131(Ar), 153 (Ar), 159 (Ar), 146 (Ar), 134 (Ar, 2C), 139 (Ar, 2C), 135 (Ar), 78.5 (OCH<sub>2</sub>),

**(3c) (E)-1-((5-bromothiophen-2-yl)methylene)thiosemicarbazide (3f)**



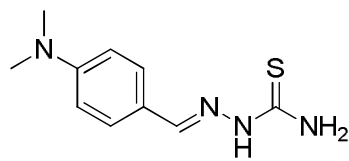
Yield:75%; M.P 243 °C R<sub>f</sub>: 0.42; Petroleum ether : ethyl acetate (6:4) **IR**; (KBr, cm<sup>-1</sup>): 3417 (NH<sub>2</sub>), 3264 (N-H), 3126(sp<sup>2</sup>CH), 1609(C=N), 1587 (Ar-C=C), 1080 (C=S), <sup>1</sup>H NMR (300 MHz, DMSO-d<sub>6</sub>): δ (ppm): 10.42 (s, 1H, NH), 7.63 (s, 1H, CH=N), 6.68 – 6.65 (m, 2H Ar-H). 6.52 (s, 2H -NH<sub>2</sub>), <sup>13</sup>C **NMR** (75 MHz, DMSO-d<sub>6</sub>): δ (ppm): 178.4, 141.6, 138.8, 132.6, 131.6, 117.1.

**(3d) (Z)-2-(4-((4-methoxybenzyl)oxy)benzylidene)hydrazinecarbothioamide**



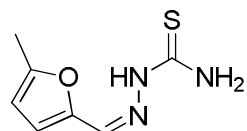
(92%) m.p 178<sup>o</sup>C; Rf: 0.58; **IR**; (KBr, cm<sup>-1</sup>): 3379 (NH<sub>2</sub>), 3235 (N-H), 1593 (CN), 1578(Ar-C=C), 1095 (C=S), cm<sup>-1</sup>; <sup>1</sup>H NMR (Acetone-d<sub>6</sub>,300 MHz) δ: 10.3 (s, 1H, NH), 8.02 (s, 1H, CH=N), 7.25-7.12 (m, 4H, ArH), 7.20-6.79 (m, 4H, ArH), 7.1 (s, 2H, -NH<sub>2</sub>), 5.70 (s, 1H, -OCH<sub>2</sub>); 3.8 (s, 3H, -OCH<sub>3</sub>); <sup>13</sup>C NMR (75 MHz) δ: 179.0 (C=S), 146(C=N), 120 (Ar), 123 (Ar), 129 (Ar), 133(Ar), 154 (Ar), 158 (Ar), 149 (Ar), 136 (Ar, 2C), 141 (Ar, 2C), 137 (Ar), 75 (OCH<sub>2</sub>), 59 (OCH<sub>3</sub>).

**(3e) (E)-2-(4-(Dimethylamino)benzylidene)hydrazine-1-carbothioamide (3a)**



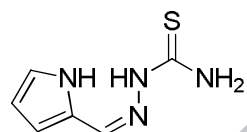
(70%): m.p 180°C;  $R_f$ : 0.46; (**IR**; (KBr,  $\text{cm}^{-1}$ ): 3374 ( $\text{NH}_2$ ), 3240 (N-H), 3125 ( $\text{sp}^2\text{-CH}$ ), 2935 ( $\text{sp}^3\text{CH}$ ), 1603 (C=N), 1587 (Ar-C=C), 1090 (C=S),  **$^1\text{HNMR}$** ; (300MHz, DMSO):  $\delta$  10.44 (s, 1H, NH), 7.07 (d,  $J = 7.5$  Hz, 2H), 6.83 (d,  $J = 7.5$  Hz, 2H), 6.75 (s, 2H,  $\text{NH}_2$ ), 2.93 (s, 6H).  **$^{13}\text{CNMR}$**  (75 MHz.):  $\delta$  181.11, 153.88, 145.68, 128.76, 120.96, 110.95, 41.90.

**(3f) (Z)-2-((5-methylfuran-2-yl)methylene)hydrazinecarbothioamide**



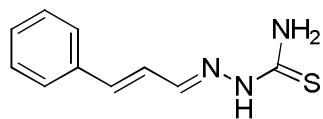
(75%): m.p 243 °C  $R_f$  : 0.42; **IR**; (KBr,  $\text{cm}^{-1}$ ): 3414 ( $\text{NH}_2$ ), 3260 (N-H), 3125( $\text{sp}^2\text{CH}$ ), 2935( $\text{sp}^3\text{CH}$ ), 1603(C=N), 1587 (Ar-C=C), 1090 (C=S), 1053(C-O);  **$^1\text{HNMR}$** ; (300MHz, DMSO):  $\delta$  10.52 (s, 1H, NH), 7.53 (s, 1H, CH=N), 7.48 (dd,  $J = 21.8, 7.5$  Hz, 2H), 7.6 (t,  $J = 7.4$  Hz, H), 7.3 (s, 2H, - $\text{NH}_2$ ); 2.20 (s, 3H).  **$^{13}\text{CNMR}$**  (75 MHz.):  $\delta$  181.11, 153.28, 146.59, 141.76, 117.91, 106.78, 14.49.

**(3g) (Z)-2-((1H-pyrrol-2-yl)methylene)hydrazinecarbothioamide**



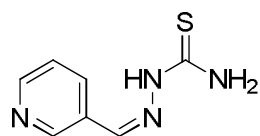
(75%): m.p 232°C  $R_f$  : 0.42; Petroleum ether : ethyl acetate (6:4) **IR**; (KBr,  $\text{cm}^{-1}$ ): 3414 ( $\text{NH}_2$ ), 3260 (N-H), 3125 ( $\text{sp}^2\text{CH}$ ), 1603 (C=N), 1587 (Ar-C=C), 1090 (C=S),  **$^1\text{HNMR}$** ; (300MHz, DMSO):  $\delta$  10.92 (s, 1H, NH), 7.53(s, 1H, CH=N), 7.05 – 6.96 (m, 2H), 6.59 – 6.51 (m, 3H), 6.26 (t,  $J = 7.5$  Hz, 1H) 6.1 (s, 2H, - $\text{NH}_2$ ); 6.0 (s, 1H, -NH);  **$^{13}\text{C NMR}$**  (125 MHz.)  $\delta$  181.11, 138.24, 124.70, 119.49, 116.23, 110.84.

**(3h) (E)-2-((E)-3-phenylallylidene)hydrazinecarbothioamide**



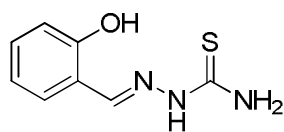
**Yield: 70%; R<sub>f</sub>: 0.63; m.p: 240°C; IR: (KBr) ( $\lambda_{\max}$ , cm<sup>-1</sup>):** 3414 (NH<sub>2</sub>), 3260 (N-H), **3075 (Ar-CH), 2930 (C-H), 1739 1715 (2 C=O), 1675, 1619 (C=N, C=C), <sup>1</sup>HNMR;** (300MHz, DMSO):  $\delta$  10.90 (s, 1H, NH), 7.53(s, 1H, CH=N), 6.59 – 6.51 (m, 5H), 6.26 (dd, 1H), 5.66 (dd, 1H) 6.1 (s,2H,-NH<sub>2</sub>); 6.0 (s, 1H, -NH); **<sup>13</sup>C NMR** (125 MHz,)  $\delta$  181.6, 138.5 ,135.70, 134.6, 128.7, 127.2, 127.3 , 126.8.

**(3i) (Z)-2-(pyridin-3-ylmethylene)hydrazinecarbothioamide**



(85%): m.p 250°C R<sub>f</sub>: 0.33; Petroleum ether : ethyl acetate (6:4) **IR;** (KBr, cm<sup>-1</sup>): 3424 (NH<sub>2</sub>), 3260 (N-H), 3135 (sp<sup>2</sup>-CH), 1605 (C=N), 1583 (Ar-C=C), 1090 (C=S), **<sup>1</sup>HNMR;** (300MHz, DMSO):  $\delta$  11.56 (s, 1H, NH), 8.90 (dd, *J* = 7.5, 1.3 Hz, 1H), 8.67 (d, *J* = 1.3 Hz, 1H), 8.26 (dt, *J* = 7.5, 1.4 Hz, 1H), 8.13 (s, 1H), 7.45 (t, *J* = 7.5 Hz, 1H), 7.40 (s, 2H NH<sub>2</sub>). **<sup>13</sup>CNMR** (75 MHz,):  $\delta$  178.2, 150.1, 148.0, 139.1, 133.9, 130.2, 123.7.

**(3j) (E)-2-(2-hydroxybenzylidene)hydrazinecarbothioamide**



**Yield:75%; M.P 235°C R<sub>f</sub> : 0.52; Petroleum ether : ethyl acetate (6:4) IR;** (KBr, cm<sup>-1</sup>): 3412 (NH<sub>2</sub>), 3250 (N-H), 3120 (sp<sup>2</sup>CH), 1608 (C=N), 1597 (Ar-C=C), 1085 (C=S), **<sup>1</sup>H NMR** (300 MHz, DMSO-*d*<sub>6</sub>):  $\delta$  (ppm): 8.05 (s, 1H, CH=N), 8.27-7.01 (m, 4H Ar-H), 7.42 (s, 2H, -NH<sub>2</sub>); 6.02 (s, 1H, OH); **<sup>13</sup>C NMR** (75 MHz, DMSO-*d*<sub>6</sub>):a  $\delta$  (ppm):.178.5, 162.9, 159.6.

General method for the preparation of methyl 2-(2-(arylidenehydrazino)-4-oxo-thiazolidin-5-ylidene)acetates (5a-j)

A thoroughly mixed uniform mixture of substituted benzylidenethiosemicarbazides **3a-j** (1.0 mmol) and dimethyl acetylenedicarboxylate **4** (142 mg, 1.0 mmol) was stirred for 1–5 min under MWI. The progress of reaction was monitored by TLC (hexane/ethyl acetate 4:1). After the reaction was completed, the solution was diluted with EtOH and the mixture was filtered. The

precipitate was recrystallized from EtOH to afford the esters **5a–j** in good yields<sup>27,28</sup>.

**2-(Furan-2-ylmethylene-hydrazono)-4-oxo-thiazolidin-5-ylidene]-acetic acid methyl ester (5a)**

Yellow Solid; Yield: 74% m.p: 276°C; **IR:** (KBr) ( $\lambda_{\max}$ ,  $\text{cm}^{-1}$ ): 3070 (Ar-CH), 2938 (C-H), 1740, 1725(2 C=O), 1673, 1630 (C=N, C=C), 1110 (C–O). <sup>1</sup>H NMR (DMSO-*d*<sub>6</sub>, 300MHz);  $\delta$  12.89 (s, 1H, N-H), 8.36 (s, 1H, CH=N), 7.94 (dd, 1H, Furan- H-5), 7.08 (d, 1H furan-H-3), 6.70 (s, 1H), 6.67 (s, 1H furan-H-4), 3.79 (s, 3H). <sup>13</sup>C NMR (DMSO, 75MHz);  $\delta$  166.80 (C-4), 165.40 (s, CO<sub>2</sub>CH<sub>3</sub>), 160.00 (s, C-2), 159.50 (CH=N), 152.00 (C-2-furan), 144.00 (C-5-furan), 142.90 (C-6), 120.00 (CH-3-furan), 114.30 (C-5), 113.00 (CH-4-furan), 61.30 (OCH<sub>3</sub>), 14.20 (CH<sub>3</sub>). **Anal.** Calcd. For C<sub>11</sub>H<sub>9</sub>N<sub>3</sub>O<sub>4</sub>S: C, 47.31; H, 3.25; N, 15.05; S, 11.48 found: C, 47.29; H, 3.27; N, 15.04; S, 11.50

**[2-[(4-Benzyloxy-benzylidene)-hydrazono]-4-oxo-thiazolidin-5-ylidene]-acetic acid methyl ester (5b)**

Yellow Solid; Yield: 70% m.p: 272°C; **IR:** (KBr) ( $\lambda_{\max}$ ,  $\text{cm}^{-1}$ ): 3080 (Ar-CH), 2948 (C-H), 1740, 1725 (2 C=O), 1658, 1636 (C=N, C=C), 1120 (C–O) <sup>1</sup>H NMR (DMSO-*d*<sub>6</sub>, 300MHz);  $\delta$  12.84(s, 1H, N-H), 8.34(s, 1H, CH=N), 7.30 – 7.19 (m, 7H), 7.14 – 6.99 (m, 2H), 6.92 (s, 1H), 5.21 – 5.17 (m, 2H), 3.87 (s, 3H). <sup>13</sup>C NMR (DMSO, 75MHz);  $\delta$  168.11, 166.5, 163.7, 163.3, 150.5, 142, 140.1, 131.5, 129.5, 130, 127.8, 126.5, 115, 114.5, 71.9, 53. **Anal.** Calcd. For C<sub>20</sub>H<sub>17</sub>N<sub>3</sub>O<sub>4</sub>S: C, 60.75; H, 4.33; N, 10.63; S, 8.11 found: C, 60.73; H, 4.36; N, 10.61; S, 8.12

**Methyl(Z)-2-((E)-2-(((E)-(5-bromothiophen-2-yl)methylene)hydrazono)-4-oxothiazolidin-5-ylidene)acetate (5c)**

Yellow Solid; Yield: 72% m.p: 278°C; **IR:** (KBr) ( $\lambda_{\max}$ ,  $\text{cm}^{-1}$ ): 3085 (Ar-CH), 2954 (C-H), 1735, 1720 (2 C=O), 1668, 1618 (C=N, C=C), 1020 (C–O) <sup>1</sup>H NMR (DMSO-*d*<sub>6</sub>, 300MHz);  $\delta$  12.75 (s, 1H, N-H), 8.43 (s, 1H, CH=N), 7.46 (dd, 1H), 6.95 (s, 1H), 6.74 (s, 1H), 3.93 (s, 3H), <sup>13</sup>C NMR (DMSO, 75MHz);  $\delta$  170.3, 169.6, 165.3, 150.5, 145.5, 143.5, 142.5, 132.5, 131.0, 116.0, 63.5. **Anal.** Calcd. For C<sub>11</sub>H<sub>8</sub>BrN<sub>3</sub>O<sub>3</sub>S<sub>2</sub>: C, 35.31; H, 2.15; N, 11.23; S, 17.13 found: C, 35.30; H, 2.16; N, 11.24; S, 17.14

**(2-[[4-(4-Methoxy-benzyloxy)-benzylidene]-hydrazono]-4-oxo-thiazolidin-5-ylidene)-acetic acid methyl ester (5d)**

Yellow Solid; Yield: 76% m.p: 232°C; **IR:** (KBr) ( $\lambda_{\max}$ ,  $\text{cm}^{-1}$ ): 3095 (Ar-CH), 2951 (C-H), 1730, 1718 (2 C=O), 1678, 1628 (C=N, C=C), 1032 (C-O)  **$^1\text{H}$  NMR** (DMSO- $d_6$ , 300MHz);  $\delta$  12.23 (s, 1H, N-H), 8.31(s, 1H, CH=N), 7.29 – 7.14 (m, 4H), 7.14 – 7.02 (m, 2H), 6.93 – 6.81 (m, 3H), 5.19 – 5.15 (m, 2H), 3.87 – 3.79 (m, 6H).  **$^{13}\text{C}$  NMR** (DMSO, 75MHz);  $\delta$  169.11, 167.5, 166.7, 164.3, 151.5, 144, 143.1, 135.5, 134.5, 130, 128.8, 125.5, 115, 113.5, 71.9, 53, 14.5. Anal. Calcd. For  $\text{C}_{21}\text{H}_{19}\text{N}_3\text{O}_5\text{S}$ : C, 59.28; H, 4.50; N, 9.88; O, 18.80; S, 7.54 found: C, 59.26; H, 4.52; N, 9.86; S, 7.56

**methyl(Z)-2-((E)-2-(((E)-4-(dimethylamino)benzylidene)hydrazono)-4-oxothiazolidin-5-ylidene)acetate (5e)**

Orange Solid Yield: 82% m.p: 245°C; **IR:** (KBr) ( $\lambda_{\max}$ ,  $\text{cm}^{-1}$ ): 3085 (Ar-CH), 2945 (C-H), 1733, 1715 (2 C=O), 1666, 1638 (C=N, C=C), 1035 (C-O)  **$^1\text{H}$  NMR** (DMSO- $d_6$ , 300MHz);  **$^1\text{H}$  NMR** (DMSO- $d_6$ , 300MHz);  $\delta$  12.80 (s, 1H, N-H), 8.53 (s, 1H, CH=N), 7.46 (dd, 2H, H-o), 6.93 (m, 2H), 6.72 (s, 1H), 3.93 (m, 3H), 2.95 – 2.91 (m, 6H).  **$^{13}\text{C}$  NMR** (DMSO, 75MHz);  $\delta$  170.4, 168.5, 164.5, 153.4, 150.7, 143.5, 131.5, 130.2, 125.4, 116.3, 55.3, 55.5 Anal. Calcd. For  $\text{C}_{15}\text{H}_{16}\text{N}_4\text{O}_3\text{S}$ : C, 54.20; H, 4.85; N, 16.86; S, 9.65 found: C, 54.18; H, 4.87; N, 16.83; S, 9.68

**{2-[(5-Methyl-furan-2-ylmethylene)-hydrazono]-4-oxo-thiazolidin-5-ylidene}-acetic acid methyl ester (5f)**

Yellow precipitates; Yield: 70% m.p: 251°C; **IR:** (KBr) ( $\lambda_{\max}$ ,  $\text{cm}^{-1}$ ): 3081 (Ar-CH), 2947 (C-H), 1740, 1723 (2 C=O), 1675, 1622 (C=N, C=C), 1112 (C-O)  **$^1\text{H}$  NMR** (DMSO- $d_6$ , 300MHz);  $\delta$  12.77 (s, 1H, N-H), 8.32 (s, 1H, CH=N), 7.94 (dd, 1H, Furan- H-5)), 7.07 (d, 1H furan-H-3), 6.74 (s, 1H), 6.68 (s, 1H furan-H-4), 3.79 (s, 3H), 2.27(s, 3H).  **$^{13}\text{C}$  NMR** (DMSO, 75MHz);  $\delta$  169.8 (C-4), 167.4 (s, CO<sub>2</sub>CH<sub>3</sub>), 163.0 (s, C-2), 159.5 (CH=N), 152.0 (C-2-furan), 146.0 (C-5-furan), 145.9 (C-6), 123.0 (CH-3-furan), 117.30 (C-5), 114.0 (CH-4-furan), 65.30 (OCH<sub>3</sub>), 14.20 (CH<sub>3</sub>). 12.20 (CH<sub>3</sub>). Anal. Calcd. For  $\text{C}_{12}\text{H}_{11}\text{N}_3\text{O}_4\text{S}$ : C, 49.14; H, 3.78; N, 14.33; S, 10.93 found: C, 49.12; H, 3.79; N, 14.34; S, 10.92

**{4-Oxo-2-[(1H-pyrrol-2-ylmethylene)-hydrazono]-thiazolidin-5-ylidene}-acetic acid methyl ester (5g)**

Brown Solid; Yield: 74% m.p: 282°C; **IR:** (KBr) ( $\lambda_{\max}$ ,  $\text{cm}^{-1}$ ): 3085 (Ar-CH), 2950 (C-H), 1742, 1725 (2 C=O), 1665, 1620 (C=N, C=C), 1012 (C-O)  **$^1\text{H}$  NMR** (DMSO- $d_6$ , 300MHz); 12.20 (s, 1H- NH), 8.34 (s, 1H, CH=N), 7.08 (d,  $J = 16.0$  Hz, 2H), 6.72 (s, 1H), 6.43 (s, 1H), 6.28 (s, 1H),

3.63 (s, 3H).  $^{13}\text{C}$  NMR (DMSO, 75MHz);  $\delta$ 173, 166.5, 165.5, 163.7, 143.5, 135.5, 133.5, 122.5, 115.4, 110.5, 60.2. Anal. Calcd. For  $\text{C}_{11}\text{H}_{10}\text{N}_4\text{O}_3\text{S}$ : C, 47.48; H, 3.62; N, 20.13; S, 11.52 found: C, 47.47; H, 3.63; N, 20.14; S, 11.53

**{4-Oxo-2-[(3-phenyl-allylidene)-hydrazono]-thiazolidin-5-ylidene}-acetic acid methyl ester (5h)**

Light orange Solid; Yield: 72% m.p: 248°C; IR: (KBr) ( $\lambda_{\text{max}}$ ,  $\text{cm}^{-1}$ ): 3075 (Ar-CH), 2930 (C-H), 1739 1715 (2 C=O), 1675, 1619 (C=N, C=C), 1042 (C-O)  $^1\text{H}$  NMR (DMSO- $d_6$ , 300MHz);  $\delta$  12.30 (s, 1H N-H), 8.28(s, 1H, CH=N), 7.59 (s, 1H), 7.35 – 7.24 (m, 3H), 7.22 (s, 1H), 7.18 (s, 1H), 6.90 (s, 1H), 6.72 (s, 1H), 3.65 (s, 3H).  $^{13}\text{C}$  NMR (DMSO, 75MHz);  $\delta$ 169.2, 167.3, 164.5, 159.0, 147.5, 145.2, 140.5, 137.4, 132.4, 130.5, 127.5, 120, 60. Anal. Calcd. For  $\text{C}_{15}\text{H}_{13}\text{N}_3\text{O}_3\text{S}$ : C, 57.13; H, 4.16; N, 13.33; S, 10.17 found: C, 57.15; H, 4.18; N, 13.37; S, 10.13.

**[4-Oxo-2-(pyridin-4-ylmethylene-hydrazono)-thiazolidin-5-ylidene]-acetic acid methyl ester (5i)**

White Solid; Yield: 78% m.p: 270°C; IR: (KBr) ( $\lambda_{\text{max}}$ ,  $\text{cm}^{-1}$ ): 3092 (Ar-CH), 2950 (C-H), 1740, 1725 (2 C=O), 1665, 1629 (C=N, C=C), 1027 (C-O)  $^1\text{H}$  NMR (DMSO- $d_6$ , 300MHz);  $\delta$  12.81(s, 1H, N-H), 8.79 – 8.68 (m, 2H), 8.04 (s, 1H, CH=N), 7.86 – 7.72 (m, 2H), 6.91 (s, 1H), 3.87 (s, 3H).  $^{13}\text{C}$  NMR (DMSO, 75MHz);  $\delta$ 168.5, 167.0, 165.0, 158.2, 153.0, 151.5, 145.2, 136.5, 128.4, 57.4. Anal. Calcd. For  $\text{C}_{12}\text{H}_{10}\text{N}_4\text{O}_3\text{S}$ : C, 49.65; H, 3.47; N, 19.30; S, 11.04 found: C, 49.60; H, 3.52; N, 19.32; S, 11.02

**{2-[(2-Hydroxy-benzylidene)-hydrazono]-4-oxo-thiazolidin-5-ylidene}-acetic acid methyl ester (5j)**

Light pink Solid; Yield: 70% m.p: 225°C; IR: (KBr) ( $\lambda_{\text{max}}$ ,  $\text{cm}^{-1}$ ): 3438 (OH), 3095 (Ar-CH), 2940 (C-H), 1736 1720 (2 C=O), 1675, 1639 (C=N, C=C), 1037 (C-O)  $^1\text{H}$  NMR (DMSO- $d_6$ , 300MHz);  $\delta$  12.06 (s, 1H N-H), 8.22 (s, 1H, CH=N), 7.40 (d,  $J = 17.3$  Hz, 2H), 7.18 (d,  $J = 8.7$  Hz, 2H), 6.91 (s, 1H), 3.85 (m, 3H), 2.96 (s, 1H).  $^{13}\text{C}$  NMR (DMSO, 75MHz);  $\delta$ 173.2, 169.6, 165.7, 163.5, 155.4, 145.5, 138.5, 132.6, 131.5, 125.5, 120.5, 118.3, 56. Anal. Calcd. For  $\text{C}_{13}\text{H}_{11}\text{N}_3\text{O}_4\text{S}$ : C, 51.14; H, 3.63; N, 13.76; S, 10.50 found: C, 51.16; H, 3.62; N, 13.75; S, 10.52

**Mushroom tyrosinase assay**

The mushroom tyrosinase (EC 1.14.18.1) (Sigma Chemical Co.) was used for in vitro bioassays as described previously with some modifications.<sup>29</sup> Briefly, 140  $\mu\text{L}$  of phosphate buffer (20 mM, pH 6.8), 20  $\mu\text{L}$  of mushroom tyrosinase (30 U/mL) and 20  $\mu\text{L}$  of the inhibitor solution were placed in the wells of a 96-well micro plate. After pre-incubation for 10 min at room temperature, 20  $\mu\text{L}$  of L-DOPA (3,4-dihydroxyphenylalanine) (0.85 mM) was added and the plate was further incubated at 25°C for 20 min. Subsequently the absorbance of dopachrome was measured at 475 nm using a micro plate reader (OPTI<sub>Max</sub>, Tunable). Kojic acid was used as a reference inhibitor and for negative tyrosinase inhibitor phosphate buffer was used instead of the inhibitor solution. The extent of inhibition by the test compounds was expressed as the percentage of concentration necessary to achieve 50% inhibition ( $\text{IC}_{50}$ ). Each concentration was analyzed in three independent experiments run in triplicate. The  $\text{IC}_{50}$  values determined by the data analysis and graphing software Origin 8.6, 64-bit.

### **Kinetic analysis of the inhibition of tyrosinase**

A series of experiments were performed to determine the inhibition kinetics by following method.<sup>30,31</sup> Different inhibitor concentrations of compound **5i** 0.00, 1.06, 8.50 and 17.00  $\mu\text{M}$ , with L-DOPA concentrations 0.062, 0.125, 0.25, 0.5, 1 and 2 mM, were taken respectively. Pre-incubation and measurement time was the same as discussed in mushroom tyrosinase inhibition assay. Maximal initial velocity was determined from initial linear portion of absorbance up to five minutes after addition of mushroom tyrosinase at a 30s interval. The inhibition type on the enzyme was assayed by Lineweaver–Burk plots of inverse of velocities ( $1/V$ ) versus inverse of substrate concentration  $1/[S]$   $\text{mM}^{-1}$ . The inhibition constant  $K_i$  was determined by two methods, the second plots of the apparent slope versus the concentration of compound **5i**, and with the help of Dixon plot. In Dixon plot different concentrations 0.0, 1.06, 2.12, 4.25, 8.5, 17 and 34  $\mu\text{M}$  of compound **5i** plot versus inverse of velocities ( $1/V$ ) with changing concentrations of L-DOPA (0.25, 0.5, 1 and 2 mM), respectively.

### **Molecular docking**

#### **Preparation of receptor**

Molecular Operating Environment (MOE 2014) was used for current studies<sup>32</sup>. The protein preparation step involved 3D protonation, energy minimization and active site identification. The

crystal structure of was obtained from protein data bank with co-crystallized ligand<sup>33</sup>. Water molecules were removed. Protein was energy minimized and 3-D protonated by using the structure preparation module of MOE. Since, the protein contains the co-crystallized ligand, so active site was identified around co-crystallized ligand by using LigX module of the MOE. The pocket was found to be deep cavity lined with the key residues including both hydrophobic and hydrophilic amino acids.

### **Preparation of Ligands**

The ligand files for molecular docking studies were prepared in Molecular Operating Environment (MOE-2014) by Chemical computing group (CCG) and were followed by energy optimization at standard MMFF94 force field level, with a 0.0001 kcal/mol energy gradient convergence criterion<sup>34</sup>. The optimized geometries were saved in molecular data base file for further studies.

### **Docking studies**

The optimized ligands were docked with the mushroom tyrosinase (PDB code: 2Y9X) protein using the MOE-Dock program. A total of 30 independent docking runs were performed using MOE docking simulation program. The docked poses were analyzed and the best scored pose for each compound was chosen for further studies of interaction evaluation. The 2D ligand-protein interactions were visualized using the MOE ligand interactions program.

### **QSAR study**

#### **Methodology**

The training set comprised of 10 compounds, tyrosinase inhibitors were used in the present QSAR study. Compound structures were optimized using molecular mechanics (MM2) implemented in ChemBio Office 2012 (Chem3D Pro 13.0) and exported to CODESSA-Pro where they were subjected to MOPAC calculation for refined final geometry optimization. CODESSA-Pro calculated 507 constitutional, topological, geometrical, quantum chemical and electrostatic descriptors for the exported bio-active scaffolds. The data set comprises training set only. To validate the model generated internal cross validation criteria was used keeping in view the small size data set.

**Multi-linear modelling**

BMLR (best multi-linear regression) was initiated stepwise to search for the best n-parameter regression equations, based on the highest  $R^2$  (squared correlation coefficient) and  $F$  (Fisher criteria) values. QSAR models with up to 2 descriptors were generated (the maximum number allowed according to the 5:1 rule of thumb, the ratio between the data points and the number of descriptors). The statistical parameters including the square of the correlation coefficient ( $R^2$ ), the squared cross-validated correlation coefficient ( $R^2_{cv}$ ), the Fisher criterion ( $F$ ) and the variance ( $s^2$ ) were used to select the best QSAR model.

**References**

1. Garbe, TR.; Kobayashi, M.; Shimizu, N.; Takesue, N.; Ozawa, M.; Yukawa, H. *J. Nat. Prod.* **2000**, 63, 596.
2. Sadaphal, SA.; Shelke, KF.; Sonar, SS.; Shingare, MS. *Cent Eur J Chem.* **2008**,6, 622.
3. Deb, ML.; Bhuyan, PJ. *Tetrahedron Lett.* **2006**, 47, 1441.
4. Sato, H.; Ishihara, S.; Kawashima, K.; Moriyama, N.; Suetsugu, H.; Kazuori, H.; Okuyama T.; Rumi, M.A.; Fukuda, R.; Nagasue, N.; Kinoshita, Y. *Br. J. Cancer* **2000**, 83, 1394.
5. Takahashi, N.; Okumura, T.; Motomura, W.; Fujimoto, Y.; Kawabata, I.; Kohgo, Y. *FEBS Lett.* **1999**, 455, 135.
6. Elgemeie, GH.; Sayed, SH. *Synthesis* **2001**, 1747.
7. Berseneva, VS.; Tkachev, AV.; Morzherin, YuYu.; Dehaen, W.; Luyten, I.; Toppet, S.; Bakulev VA. *J Chem Soc, Perkin Trans.* **1998**,1, 2133.
8. Mishra, S.; Ghosh, R. *Indian J Chem.* **2011**, 50B, 1630.
9. Hasaninejad, A.; Zare, A.; Sharghi, H.; Niknam, K.; Shekouhy, M. *ARKIVOC.* **2007**, xiv, 39.
10. Pan, K.; Scott, MK.; Lee, DHS.; Fitzpatrick, LJ.; Crooke, JJ.; Rivero, RA.; Rosenthal, DI.; Vaidya, AH.; Zhao, B.; Reitz, AB. *Bioorg Med Chem.* **2003**, 11, 185.
11. De la Hoz, A.; Loupy, A. editors. *Microwaves in organic synthesis.* 3rd ed., 2 vols. Weinheim:Wiley-VCH; **2012**.
12. Aly, AA.; Ahmed, EK.; El-Mokadam, KM. *J Heterocycl Chem.* **2007**, 44, 1431.
13. Aly, AA.; Brown, AB.; Abdel-Aziz, M.; Abuo-Rahma, GEAA.; Radwan, MF.; Ramadan, M.; Gamal-Eldeen, AM. *J Heterocycl Chem.* **2012**, 49, 726.
14. Aly, A. A.; Brown, A. B.; Abdel-Aziz, M.; Abuo-Rahma, G. E. A.A.; Radwan, M. F.; Ramadan, M.; Gamal-Eldeen, A. M. *J Heterocycl Chem*, **2010**, 47, 547.
15. Aly, A. A.; Hassan, A. A.; Ibrahim, Y. R. *J Chem Res* **2008**, 699.
16. Manaka, A.; Ishii, T.; Takahashi, K.; Sato, M. *Tetrahedron Lett* **2005**, 46, 419.
17. Kodomari, M.; Suzuki, M.; Tanigawa, K.; Aoyama, T. *Tetrahedron Lett* **2005**, 46, 5841.
18. Hartung, J.; Rosenbaum, K.; Beyer, L.; Losada, J.; Fernandez, V. *J prakt Chem* **1991**, 333, 537.
19. Zeng, R.-S.; Zou, J.-P.; Zhi, S.-J.; Chen, J.; Shen, Q. *Org Lett* **2003**, 5, 1657.
20. Hassan, A. A.; Ibrahim, Y. R.; Aly, A. A.; El-Sheref, E. M.; Yamato, T. *J Heterocycl Chem* **2011**, 48, 2012.

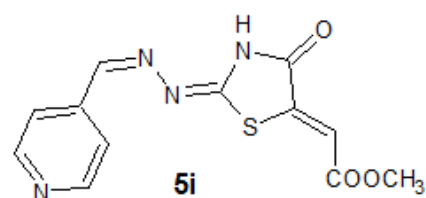
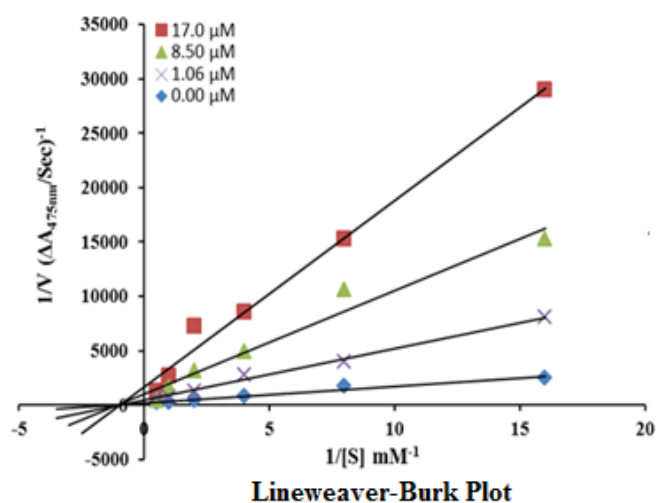
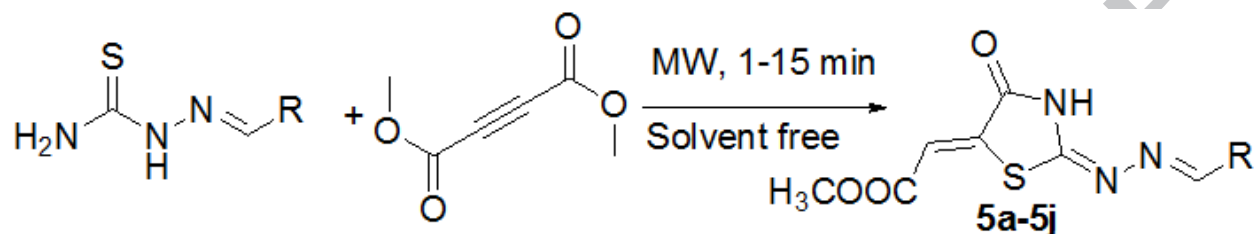
21. Yu, K.; Masahiko, I.; Takayasu, Y.; Kimio, H.; Noriko, T. *Bioorg Med Chem* **2014**, *22*, 3994.
22. Wang-Chuan, C.; Tien-Sheng, T.; Nai-Wan, H.; Yun-Lian, L.; Zhi-Hong, W.; Chin-Chuan, T.; Yu-Ching, L.; Hui-Hsiung, L.; Keng-Chang, T. *Scientific Reports*, **2014**, *5*, 7995.
23. Kowsar, B.; Faezeh, ST.; Amirhossein, S.; Mohammad, R. *J Biomol Structure and Dynamics*, **2015**, *33*, 487.
24. Young, MH.; Yun, JP.; Jin-Ah, K.; Daeui, P.; Ji, YP.; Hye, JL.; Ji, YL.; Hyung, RM.; Hae, YC. *Eur J Med Chem* **2012**, *49*, 245.
25. Saeed, A., Al-Masoudi, N.A. and Latif, M., Synthesis and Antiviral Activity of New Substituted Methyl [2-(arylmethylene-hydrazino)-4-oxo-thiazolidin-5-ylidene] acetates. *Archiv der Pharmazie*, 346, **2013**, 625.
26. Saeed, A., Imran, A., Channar, P.A., Shahid, M., Mahmood, W., Iqbal, J., 2-(Hetero (aryl) methylene) hydrazine-1-carbothioamides as Potent Urease Inhibitors. *Chem Bio Drug Design*, **2015**, *85*, 230.
27. Darehkordi, A., Saidi, K. and Islami, M.R., 2007. Preparation of heterocyclic compounds by reaction of dimethyl and diethyl acetylene dicarboxylate (DMAD, DEAD) with thiosemicarbazone derivatives. *Arkivoc*, *1*, 180-188.
28. Aly, A.A., Ishak, E.A. Brown, A.B., Reaction of arylidenehydrazono-4-aryl-2, 3-dihydrothiazole-5-carbonitriles with diethyl acetylenedicarboxylate. Synthesis of (Z)-ethyl 2-[(Z)-2-(E)-arylidenehydrazono)-4-oxo-thiazolidine-5-ylidene] acetates. NMR investigation. *J Sulf Chem*, **2014**, *35*, 382-393.
29. Ashraf, Z.; Rafiq, M.; Seo, SY.; Babar, MM.; Zaidi, NSS. *Bioorg. Med. Chem.* **2015**, *23*, 587.
30. Woo, DS.; Young, BR.; Marcus, JC.; Chan, WL.; Hyung, WR.; Ki CJ.; Ki, HP. *Eur. J. Med. Chem.* **2010**, *45*, 2010.
31. Ashraf, Z.; Rafiq, M.; Seo, SY.; Babar, MM.; Zaidi, NSS. *J Enzyme Inhib Med Chem.*, **2015**, *30*, 874.

32. Molecular Operating Environment (MOE), 2013.08; Chemical Computing Group Inc., 1010. Sherbooke St. West, Suite #910, Montreal, QC, Canada, H3A 2R7, 2015.
33. Ismaya, WT.; Rozeboom, HJ.; Weijn, A.; Mes, JJ.; Fusetti, F.; Wichers, HJ.; Dijkstra, BW. *Biochemistry*, **2011**, 50, 5477.
34. Halgren, TA. *J. Comput. Chem.* **1996**, 17, 587.

ACCEPTED MANUSCRIPT

Synthesis, computational studies and enzyme inhibitory kinetics of substituted methyl[2-(4-dimethylamino-benzylidene)-hydrazono]-4-oxo-thiazolidin-5-ylidene]acetates as mushroom tyrosinase inhibitors

## Graphical Abstract



$\text{IC}_{50} 3.17 \pm 0.37 \mu\text{M}$

**Non-competitive Inhibitor**

**Kinetic and *in silico* studies of novel hydroxy-based thymol analogues as inhibitors of mushroom tyrosinase**

- Hydroxylated thymol analogues (**4a-4e**) and (**6a-6c**) were efficiently synthesized.
- Compound (**6b**) showed highest tyrosinase inhibitory activity ( $IC_{50}$  15.20 $\mu$ M).
- Kinetic analysis revealed (**6b**) is mixed type inhibitor ( $K_i$  25 $\mu$ M).
- Compound (**6b**) formed reversible enzyme-inhibitor complex.
- The compound (**6b**) also well docked with protein (PDBID 2ZMX).